Magnetic Flux Conversion and the Importance of Tearing Modes in the DIII-D Advanced Inductive Scenario*

N.Z. Taylor[1], T.C. Luce[2], R.J. La Haye[2], C.C. Petty[2]

[1] *Oak Ridge Associated Universities, Oak Ridge, TN, USA*

[2] *General Atomics, San Diego, CA , USA*

Introduction

The advanced inductive (AI) scenario is an easily attainable, stationary regime that has higher confinement and greater stability to the m/n=2/1 Neoclassical Tearing Mode (NTM) compared to the conventional H-mode regime [1]. A key feature of the AI scenario is the anomalous transport of poloidal flux that produces an anomalously broad current profile which raises the minimum safety factor (q_{min}) above one. The physical mechanism involved in this flux pumping that keeps $q_{min} > 1$ is not understood. A well established result on DIII-D is that a tearing mode (usually a m/n=3/2 mode) is present when the flux pumping is observed [2]. One hypothesis is that the time-asymmetric modulation of the tearing mode amplitude by Edge Localized Modes (ELMs) or other transient MHD modes (such as fishbones) is responsible for the transport of poloidal flux [3]. Recent simulations and experiments have shown that the presence of a helical core could produce a dynamo EMF that broadens the current profile [4, 5]. In these simulations and experiments the current broadening is being facilitated by a core n=1 mode. The connection between a core n=1 mode and the 3/2 tearing mode has not been established. It is possible that in AI plasmas the 3/2 tearing mode is driving a 2/2 sideband that produces a helical core and is driving the flux pumping [6].

Flux states as a tool to track poloidal flux consumption

Flux states are scalar energies, normalized by the plasma current, that can be used to track the energy flow from the poloidal field coils of a tokamak to the electromagnetic and kinetic stored energy of the plasma. Flux states have been applied to determine the optimal flux usage in current and future devices [7]. The coil and kinetic flux states are defined as $\Psi_c I_p = W_c$ and $\Psi_{kin} I_p = W_{kin}$, where W_c is the amount of energy coupled between the poloidal field coils and the plasma and W_{kin} is the amount of magnetic energy converted to kinetic energy by the electric field within the plasma.

The analysis in the following section tracks the rate poloidal flux is provided by the coils and converted to kinetic energy by evaluating the time rate change in flux states during the stationary period of the discharge; results are reported in Webers/second or Volts. These rates are defined

in Eq. (1) and Eq. (2).

$$\frac{\mathrm{d}\Psi_c}{\mathrm{d}t} = \frac{1}{I_p}\frac{\mathrm{d}W_c}{\mathrm{d}t} = \frac{1}{I_p}\int \mathrm{d}R\mathrm{d}z\frac{\mathrm{d}}{\mathrm{d}t}\left(J_\phi\,\psi_c\right) \tag{1}$$

$$\frac{\mathrm{d}\Psi_{kin}}{\mathrm{d}t} = \frac{1}{I_p}\frac{\mathrm{d}W_{kin}}{\mathrm{d}t} = \frac{1}{I_p}\int \mathrm{d}R\mathrm{d}zJ_\phi\frac{\mathrm{d}\psi}{\mathrm{d}t} \tag{2}$$

where ψ_c, J_ϕ, and ψ are the poloidal vacuum flux applied by the coils, the toroidal current density, and the total poloidal flux respectively. ψ_c is calculated at each time slice from the measured currents in each of the 18 poloidal field coils and the central solenoid coil and their known geometries in DIII-D. J_ϕ, and ψ are calculated at each time slice by EFIT, a 2D equilibrium reconstruction code. EFIT is given experimental data (external magnetic probes, external flux loops, internal motional Stark effect magnetic pitch angle profile) measurements and returns the best estimate of the poloidal flux $\psi(R,z)$ that satisfies the Grad-Shafranov equation.

Dependence of flux conversion on high beta and presence of 3/2 tearing mode

A series of AI discharges were produced in DIII-D. These were double null, H-mode plasmas with the plasma current I_p = 1.2 MA and vacuum toroidal field B_T= 1.89 T. The safety factor at the 95% flux surface q_{95}=4.5, which is in the typical operating regime for advanced inductive scenario in DIII-D. The normalized plasma pressure, $\beta_N = \beta(\%)/[I(MA)/a(m)B(T)]$, was $\beta_N \sim$ 2.6. As is typical in these AI plasmas in DIII-D, nearly all of these discharges had a m/n=3/2 TM. The few cases where there was no 3/2 TM present there was a 4/3 mode. Electron Cyclotron Current Drive (ECCD) was applied to the q=1.5 surface to drive current in the co-Ip direction to suppress the TM or the counter Ip direction to destabilize the TM further. These shots were compared to cases where Electron Cyclotron Resonant Heating (ECRH) was applied to the q=3/2 surface so it has the same heating as the ECCD cases, but no current driven to affect the size of the TM.

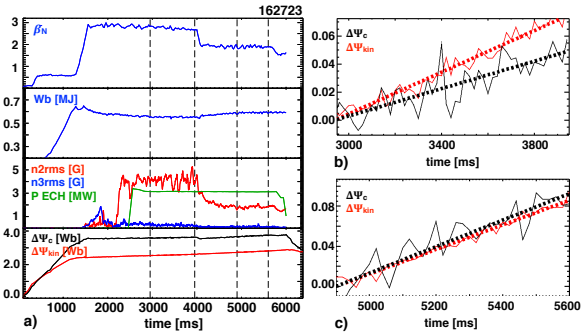

Figure 1: *a) Time traces from an AI discharge where the neutral beam power was reduced at 4 seconds. b) Change in the flux states during a stationary, high β_N interval. c) Change in the flux states during a stationary, low β_N interval*

Stationary intervals were identified by times in the discharge where the stored energy in the poloidal magnetic field (W_b), β_N, and tearing mode amplitude (as measured by the RMS amplitude of a Mirnov probe array) were relatively unchanged. The stationary intervals typically occurred during the last 1-2 seconds of the I_p flat-top.

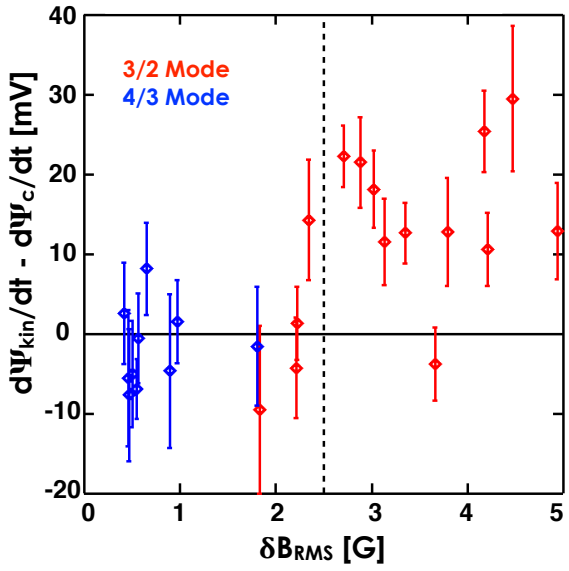

Figure 2: *a) The observed difference in the change in the kinetic and coil flux states for series of AI discharges with different tearing mode amplitudes.*

The average rate of change of the flux states during these stationary intervals was determined by fitting a line and evaluating the slope. This assumes that the flux states are advancing at a constant rate during the intervals. Shown in Figure 1 are time traces of β_N, W_b, n=2 and n=3 magnetic fluctuation amplitude, ECH power, and the flux states for an AI discharge where the injected neutral beam power was reduced at 4 seconds lowering both β_N and the 3/2 TM amplitude for the last 2 seconds of the discharge. There is an observed deficit in the rate of change of the coil and kinetic flux states in the early stationary period with a large 3/2 tearing mode present at high β_N. In the stationary interval after 4 seconds with a smaller 3/2 mode and lower β_N, no inequality in the flux states is observed.

In AI discharges where the 3/2 mode is suppressed by co-ECCD aimed at the q=3/2 rational surface, the change in the coil and kinetic flux states in stationary intervals are equal. In AI discharges where counter-ECCD was applied at the q=3/2 rational surface to amplify the 3/2 TM there is an inequality in the rate of change of the flux states during the stationary interval. The time rate of change of Ψ_{kin} is approximately 20 mV larger than Ψ_{coil} during these intervals. Similar results were observed in cases where ECH was applied to the 3/2 rational surface but no current driven and in cases in which the ECCD was poorly aimed and did not appear to effect the mode amplitude. 25 stationary intervals of approximately 1 second or longer where identified during 21 AI discharges.

Figure 2 shows the observed difference in the rate of change in the flux states ($d\Psi_{kin}/dt$-$d\Psi_{coil}/dt$) vs the median value of the tearing mode amplitude as determined by the root mean squared (RMS) amplitude of the perturbed poloidal field measured by an array of Mirnov coils on the outer vessel wall for each of the intervals. In the cases where the 3/2 TM was successfully suppressed, or in some cases where it was never present, a much smaller m/n=4/3 tearing mode emerged. The error bars in the flux state deficits in figure 2 are determined by uncertainties in the linear fitting of the slopes. As can been seen in the figure, almost any deficit < 10 mV is not statistically different from 0. The only cases with significant difference in the rate of change of flux states ($d\Psi_{kin}/dt$-$d\Psi_{coil}/dt > 10$ mV) occur when there is a > 2.3 G 3/2 mode present.

Figures 1 and 2 show that observing a deficit in the rate of change of flux states appears to be dependent on both β_N and having a sufficiently large TM present. This multi-variable dependence of the observed difference in the flux states is shown in figure 3. A significant (>10 mV) inequality is only observed in the upper right quadrant where both β_N and TM mode amplitude are large ($\beta_N > 2.25$ and $\delta B_{RMS} > 2.3$ G). No interval in the other three quadrants produced a significant deficit in the flux states.

In order to show that the AI intervals with the inequality in flux states had broader current profiles, the average normalized internal inductance (ℓ_i) was evaluated for every interval. ℓ_i is a ratio of the volume-averaged poloidal magnetic energy density and the square of the average poloidal field on the last closed flux surface. A broader current profile will result in a lower ℓ_i. In intervals where there is a flux state inequality the mean ℓ_i is 0.89 with a standard deviation $\sigma = 0.02$. In all other intervals with no flux state inequality, the mean ℓ_i is 0.93 (σ=0.03).

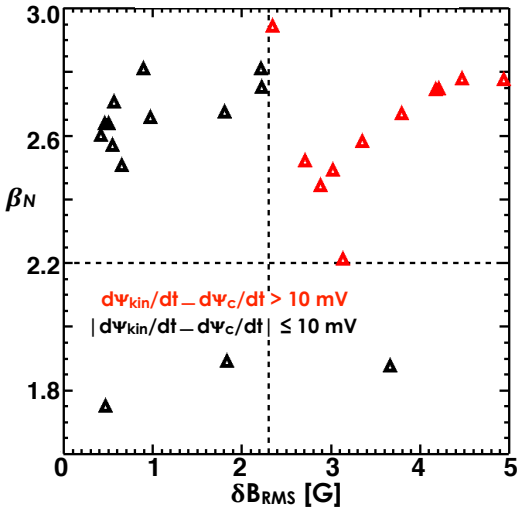

Figure 3: *The observed inequality in the evolution of flux states in stationary AI intervals vs TM amplitude and β_N.*

Conclusions

In DIII-D advanced inductive scenario discharges, a difference in the rate of change of the flux states was observed indicating the rate of poloidal magnetic energy consumption is more than the rate of energy flow from the poloidal field coils. This inequality was only present in stationary AI intervals in which a large 3/2 tearing mode was present. This supports the observation that the tearing mode is a key component of the flux pumping mechanism. An inequality in the evolution of the flux states can be used as a method of detecting flux pumping.

*This work is supported by the US DOE under DE-FC02-04ER54698 and DE-AC05-06OR23100.

References

[1] T. Luce, *et al*, Nuclear Fusion **54**, 013015 (2014)

[2] M. Wade, *et al*, Nuclear Fusion **45**, 407-416 (2005)

[3] C. Petty, *et al*, Phys. Rev. Lett. **102**, 045005 (2009)

[4] S. Jardin, N. Ferraro, and I. Krebs, Phys. Rev. Lett. **115**, 215001 (2015)

[5] P. Piovesan, *et al*, PPCF. **59**, 014027 (2017)

[6] P. Politzer, Proc. 32nd EPS-CPP, O1.001 (2005)

[7] T. Luce, *et al*, Nuclear Fusion **54**, 093005 (2014)